A REMPI and ZEKE Spectroscopic Study of *trans*-Acetanilide·H_2O and Comparison to Ab Initio CASSCF Calculations

Susanne Ullrich and Klaus Müller-Dethlefs*

Department of Chemistry, The University of York, Heslington, York, YO10 5DD U.K.

Received: December 31, 2001; In Final Form: July 9, 2002

In this paper, two-color REMPI (resonance enhanced multiphoton ionization) and ZEKE (zero kinetic energy photoelectron) spectra of the *trans*-acetanilide·H_2O complex are presented, extending our previous work on the *trans*-acetanilide monomer (Ullrich, S.; Muller-Dethlefs, K. *J. Phys. Chem. A* **2002**, *106*, 9181). Spectral features are interpreted with the aid of ab initio CASSCF/cc-pVDZ calculations and compared to the monomer and related molecular systems, such as *trans*-formanilide·H_2O (Ullrich, S.; et al. *Phys. Chem. Chem. Phys.* **2002**, *4*, 2897). In addition, the nature of the excess charge distribution in *trans*-acetanilide$^+$, and its modification upon solvation are discussed. Complexation of acetanilide with water leads to drastic changes in the S_0 and S_1 state barrier heights for methyl group internal rotation and possibly reorientation of the methyl group compared to the monomer. Observations are interpreted by simulations of methyl rotor states in a V_3-V_6 potential.

1. Introduction

Within peptides, amide groups preferably align in a trans arrangement and can therefore be modeled by *trans*-*N*-phenylamides. However, of particular interest is also solvation with water, which is not only present as a surrounding bulk but also as a ligand attached to specific binding sites in the interior of a protein. Numerous studies are available on the related neutral and cationic formanilide and its singly hydrated complex.[1−8] Hydrogen-bonded complexes of *trans*-acetanilide, which in contrast to formanilide has the peptide bond in a more centered linking position, have not been studied to our knowledge. The acetanilide monomer allows the docking of a water molecule to a more enclosed NH binding site to be investigated; additionally, the effect of solvation on the properties of the monomer species can be studied. Of interest are, for example, changes in charge distributions of the peptidic side chain, barrier heights for methyl group rotation, and side-chain torsion and complex isomer ratios.

Two-photon resonant spectroscopic techniques in combination with a supersonic jet expansion represent powerful tools for the investigation of molecular complexes. Time-of-flight discrimination allows the study of mass-selected molecular complexes, and intermediate resonances can be used to state-select specific isomers. The results obtained using such spectroscopic techniques on *trans*-acetanilide·H_2O are presented in this paper. REMPI and ZEKE spectra of the NH-bound water complex of acetanilide are obtained and interpreted using CASSCF/cc-pVDZ ab initio calculations and simulations of methyl group internal rotations.[9] In addition, the possible presence of a second, probably CO-bound, isomer of singly hydrated acetanilide in the REMPI spectrum is discussed.

2. Experimental and Computational Details

The experimental procedure has been described in detail in the monomer study and previous work and will only be summarized briefly here.[10] Acetanilide (Aldrich, 97% purity) was heated to 140 °C in a sample holder located directly behind the valve. The Ne carrier gas was passed through a water reservoir cooled in an ice−water bath and then expanded in a supersonic jet together with the monomer vapor. The molecular beam interacts with two counter propagating, frequency-doubled outputs of an excimer-pumped two-color dye laser system. The pulses employed to extract REMPI ions or ZEKE electrons were the same as in refs 10and 5.

Ab initio CASSCF calculations were performed in the same manner as described in the monomer paper using Gaussian 98[12] on an IBM RS6000. The HF molecular orbitals included in the active space consisted of the six benzene type π orbitals and the oxygen and nitrogen lone pairs of a″ symmetry: a (10/9,8) active space.[13] No orbitals from the water moiety were included.[3,14]

Optimized structures from the monomer were used as a starting geometry with the water molecule attached to the NH binding site and the methyl group in different orientations. This complex geometry is assumed to be the most stable from studies on similar systems and only calculations of this isomer were pursued further.[5,6]

3. Results and Discussion

3.1. CASSCF ab Initio Calculations. The CASSCF calculations predict that *trans*-acetanilide·H_2O adopts a C_s symmetry structure in all three states (S_0, S_1, and D_0), where two methyl hydrogens and the water hydrogens are above and below the molecular symmetry plane. In the neutral states, one methyl hydrogen faces the oxygen of the water moiety, whereas in the cation, the methyl group is rotated by 60°; that is, one methyl hydrogen is oriented toward the amide oxygen. The orientation of the methyl group in the complex therefore differs from the orientation in the acetanilide monomer in the S_0 and S_1 state. The optimized ab initio geometric structures of *trans*-acetanilide·H_2O are displayed in Figure 1 with the intermolecular geometric parameters. Full geometries are available as Supporting Infor-

* To whom correspondence should be addressed. E-mail: kmd6@york.ac.uk. Fax: +44 1904 432516.

10.1021/jp014684o CCC: $22.00
Published on Web 09/13/2002

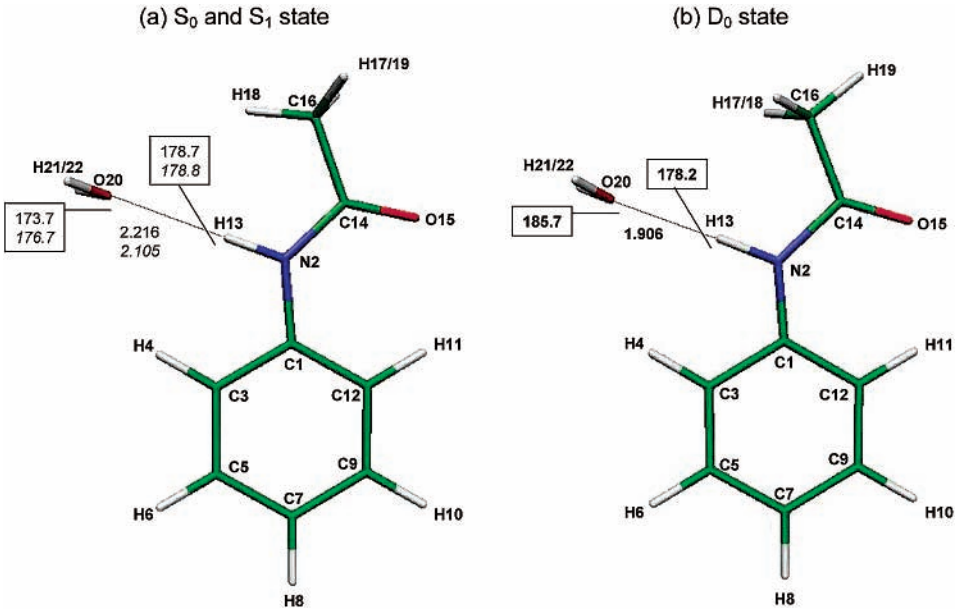

Figure 1. CASSCF/cc-pVDZ optimized geometry of *trans*-acetanilide·H_2O including labeling of atoms. Geometric parameters of the side-chain and hydrogen bond are given for the (a) S_0 (normal), S_1 (italic), and (b) D_0 (bold) states. Note: The orientation of the methyl group changed in the cationic complex compared to the neutral.

mation in Table A; excitation and ionization energies are given in Table B; and CASSCF harmonic vibrational frequencies up to 1000 cm^{-1} are listed in Table C. It should be noted that for acetamide the orientation of the methyl group showed a strong dependence on the level of theory and basis set used.[15] The issue of methyl group alignment in acetanilide·H_2O could not be investigated further; only relatively low levels of theory and calculation with small basis sets were computationally feasible.

Geometric structures of the side chain are very similar in both the monomer and complex. In the complex, bond distances and angles are slightly smaller except the C14−O15 bond and N2−C14−O15 angle, but all parameters undergo similar changes upon excitation and ionization. Upon excitation, CASSCF predicts only minor changes in side-chain bond distances and angles of acetanilide·H_2O, which become considerably more pronounced in the cation. These geometry changes mainly correspond to displacements along the in-plane bending, B′, and side-chain stretching, Σ′, coordinates. The hydrogen-bond distance is longer than in the related formanilide·H_2O but shows similar trends upon excitation and ionization. In acetanilide·H_2O, the H13···O20 bond distance shortens from 2.216 Å (S_0) to 2.105 Å (S_1) and then further to 1.906 Å (D_0). The angle between the C_{2v} axis of the water and the hydrogen bond increases upon excitation from 173.7° to 176.7° and again upon ionization to 185.7°. Because of these large geometry changes of the hydrogen bond, the intermolecular in-plane bend, β', stretch, σ, and possibly γ' are expected to be relatively prominent in REMPI and ZEKE spectra.

Partial atomic charges (Supporting Information, Table D) were calculated to investigate the nature of the excess charge distribution in the *trans*-acetanilide$^+$ moiety and its modifications upon complexation. In the cationic monomer,[13] 40% of the positive excess charge delocalizes onto the side chain (32% onto the amide group itself). Acetanilide·H_2O shows similar charge delocalization (42%), and it can be concluded that hydration of the amide group with water does not influence the overall ability for electron density redistribution. This is in line with the almost identical geometry changes upon excitation and ionization in the acetanilide monomer and the acetanilide moiety in the complex. Locally at the hydrogen bonding site, N2 is slightly more negative, whereas H13 is more positive compared to the acetanilide monomer.

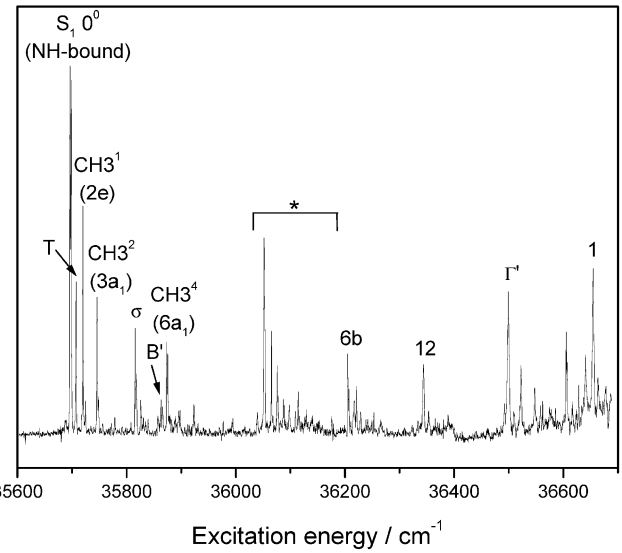

Figure 2. Two-color (1+1′) REMPI spectrum of *trans*-acetanilide·H_2O recorded with the ionization laser set to 28 820 cm^{-1}. The asterisk (*) indicates a region of fragmentation of higher clusters; see text for details.

3.2. REMPI Spectrum of *trans*-Acetanilide·H_2O. The two-color (1+1′) REMPI spectrum of acetanilide·H_2O with the ionization laser set to 28 820 cm^{-1} is displayed in Figure 2, and spectral features observed are listed in Table 1, which includes assignments and a comparison to ab initio CASSCF/cc-pVDZ harmonic frequencies.

The REMPI spectrum can be divided into two parts. The low-frequency region represents the NH-bound water complex of acetanilide with an excitation energy for the S_1 0^0 band of 35697 ± 2 cm^{-1}, corresponding to a red shift of 207 ± 2 cm^{-1}. [No distinction has been made between $0a_1$ and 1e symmetry components. Instead an absolute error of ±2 cm^{-1} is given.] This compares to a CASSCF predicted excitation energy and red shift of 37915 and 31 cm^{-1} (CASMP2+ZPE predicts 36661 cm^{-1} and −2 cm^{-1}), respectively. It should be noted that red

TABLE 1: Vibrational Features Observed in the (1+1′) REMPI Spectrum of *trans*-Acetanilide·H_2O Together with Assignments and CASSCF/cc-pVDZ Harmonic Frequencies of the S_1 State[a]

peak position/ cm^{-1}	splitting/ cm^{-1}	relative position/ cm^{-1}				assignment	CASSCF
35696.2 s	2.3	0	−2.3			$S_1 0^0$ ($0a_1$)	
35698.5 s		2.3	0			$S_1 0^0$ (1e)	
35707.3 m		11.1	8.8			T	37
35719.7 s		23.5	21.2			$CH3^1$ (2e)	65
35724.8 vw		28.6	26.3			$CH3^1+\beta''$	
35745.8 m	3.1	49.6	47.3			$CH3^2$ ($3a_1$)	
35748.9 vw		52.7	50.4			?	
35778.5 vvw		82.3	80.0			$CH3^2$ (4e)	
35815.8 m	2.1	119.6	117.3			$\sigma \leftarrow S_0\ 0^0$ ($0a_1$)	130
35817.9 w		121.7	119.4			$\sigma \leftarrow S_0\ 0^0$ (1e)	
35825.7 vvw		129.5	127.2			$CH3^3$ (5e)	
35830.9 vvw		134.7	132.4			$CH3^3+\beta''$	
35835.0 vvw		138.8	136.5			$CH3^3+\beta''^2$	
35839.0 vvw		142.8	140.5			$CH3^3+\beta''^3$	
35863.4 vw	2.1	167.2	164.9			$B'\leftarrow S_0\ 0^0$ ($0a_1$)	191
35865.5 vw		169.3	167.0			$B'\leftarrow S_0\ 0^0$ (1e)	
35873.3 w	2.4	177.1	174.8			$CH3^4$ ($6a_1$)	
35875.7 w		179.5	177.2			?	
35895.5 vvw	2.4	199.3	197.0			?	
35897.9 vvw		201.7	199.4			?	
35922.9 vvw		226.7	224.4			?	
36037.5 vvw	2.1	341.3	339.0			2B′	
36039.6 vvw		343.4	341.1			2B′	
36051.7 m	1.3	355.5	353.2	0		$S_1 0^0$ [b]	
36053.0 m		356.8	354.5	2.3	0	$S_1 0^0$ [b]	
36065.4 m	2.9	369.2	366.9	13.7	12.4	*b*	
36068.3 vw		372.1	369.8	16.6	15.3	*b*	
36076.2 w	1.1	380.0	377.7	24.5	23.2	*b*	
36077.3 w		381.1	378.8	25.6	24.3	*b*	
36087.3 vw	1.3	391.1	388.8	35.6	34.3	*b*	
36088.6 vw		392.4	390.1	36.9	35.6	*b*	
36089.9 vw		393.7	391.4	38.2	36.9	*b*	
36098.1 vvw		401.9	399.6	46.4	45.1	*b*	
36109.5 vvw		413.3	411.0	57.8	56.5	*b*	
36114.8 vw	1.5	418.6	416.3	63.1	61.8	*b*	
36116.3 vvw		420.1	417.8	64.6	63.3	*b*	
36205.0 m	2.4	508.5	506.2	153.0	151.7	6b ($0a_1$)	583
36207.4 w		511.2	508.9	155.7	154.4	6b (1e)	
36217.3 w		521.1	518.8	165.6	164.3		
36221.3 w		525.1	522.8	169.6	168.3		
36228.7 vw		532.5	530.2	177.0	175.7		
36253.2 vw		557.0	554.7	201.5	200.2		
36343.9 w		647.7	645.4	292.2	290.9	12	691
36353.3 vvw		657.1	654.8	301.6	300.3		
36499.2 m		803.0	800.7	447.5	446.2	Γ′	854
36522.7 w		826.5	824.2	471.0	469.7		
36547.6 vw		851.4	849.1	495.9	494.6		
36605.5 w		909.3	907.0	553.8	552.5		
36640.6 vw		944.4	942.1	588.9	587.6		
36654.7 m		958.5	956.2	603.0	601.7	1	1031
36663.3 vvw		967.1	964.8	611.6	610.3		

[a] All frequencies are given in cm^{-1} with an absolute error of ± 0.2 cm^{-1} and intensities denoted as vvw = very, very weak, vw = very weak, w = weak, m = medium, s = strong. Ring modes are labelled according to Wilson notation.[16] [b] Fragmentation of higher clusters.

shifts are extracted from the CASSCF calculation as a difference between two comparably large energies. Shifts are extremely difficult to calculate especially when the excited state is involved.[14]

Methyl group rotational excitation, low-frequency side-chain modes and intermolecular vibrations follow the dominant $S_1\ 0^0$ band which will be discussed later. In the higher frequency part of the REMPI spectrum, intramolecular aromatic ring vibrations are observed. Suggested assignments use the Wilson notation[16] by comparison to phenol,[17] but many such ring modes show strong coupling to displacements of the side chain, and labels should only be seen as a guide. Smaller features to the blue of those ring modes indicate that low-frequency vibrations observed on the $S_1\ 0^0$ band are repeated as combination bands, though the signal-to-noise ratio is too low to allow detailed analysis of those features.

Between these spectral regions, from ∼36 050 to ∼36 150 cm^{-1}, an additional series of peaks appears with a possible second $S_1\ 0^0$ origin band at 36 052 ± 0.2 cm^{-1} and vibrational features as listed in Table 1. An unambiguous identification of those peaks is at present not possible; however, the following observations were made: (i) It was not possible to record a ZEKE spectrum via the peak at 36 052 ± 0.2 cm^{-1}. (ii) Detailed spectroscopic measurements of formanilide·$(H_2O)_n$ clusters by Simons et al.[7] using spectral hole-burning techniques allowed them to identify a group of features ∼300 cm^{-1} above the $S_1\ 0^0$ origin. A relatively strong feature that was followed by smaller peaks could be assigned to fragmentation of the $n = 2$

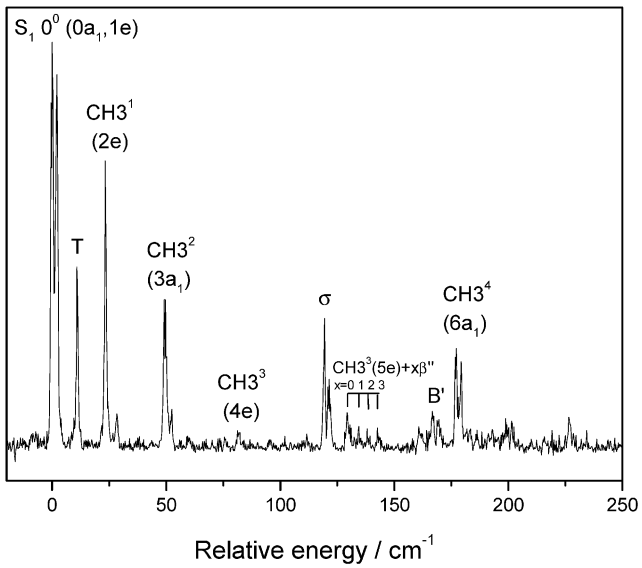

Figure 3. Two-color (1+1′)-REMPI spectrum of the low-frequency range of NH-bound *trans*-acetanlide·H_2O recorded with the ionization laser set to 28 820 cm^{-1}. The spectrum is presented relative to the S_1 0^0 ($0a_1$). Additional assignments are listed Table 1.

complex into the $n = 1$ mass channel. Furthermore, a low intensity peak and vibrations built off it could be attributed to the presence of a second, blue shifted CO-bound formanilide·H_2O isomer. Comparison to this study suggests that the peaks observed in the acetanilide·H_2O spectrum in this frequency range are also either from fragmentation of higher water clusters of acetanilide or represent the CO-bound water complex with the water acting as a proton donor. This would correspond to a blue shift of 148 ± 0.2 cm^{-1} with respect to the acetanilide monomer and is comparable to the blue shift observed for CO-bound *trans*-formanilide·H_2O (118 cm^{-1}). The time-of-flight (TOF) mass spectrum did not reveal the presence of any higher clusters even when the excitation laser was set resonant to the second origin peak; however, this could be interpreted as 100% fragmentation efficiency. (iii) The signal intensity of those peaks showed a strong dependence on the amount of one-color contribution to the (1+1′) REMPI spectrum. An increase in one-color contribution lead to a broad background in this spectral range, and peaks gained intensity. It can therefore be concluded that spectral features within this range are not related to the red shifted S_1 0^0 origin band of the NH-bound water complex of acetanilide, and fragmentation of higher clusters is considered as their most likely origin. Further hole-burning experiments could be used to confirm this conclusion.

The low-frequency part of the NH-bound acetanilide·H_2O spectrum is displayed in Figure 3. The origin band shows two components originating from population of the $0a_1$ and 1e methyl rotor states in the neutral ground state. Comparison of band profiles in Figure 4 of the two S_1 0^0 components (Figure 4a) to the contours of higher rotor states of identified symmetry and to the acetanilide monomer suggests that the $0a_1$ and 1e species occur at 35 696.2 ± 0.2 and 35 698.5 ± 0.2 cm^{-1}, respectively. This corresponds to a splitting of the S_1 0^0 band of 2.3 ± 0.2 cm^{-1}. The appearance of the two symmetry components in this order, i.e., the S_1 CH3°($0a_1$) ← S_0 $CH3_0$-($0a_1$), occurs at lower frequency as the S_1 CH3°(1e) ← S_0 $CH3_0$-(1e), implies that the barrier in the ground state is higher than in the excited state. The opposite observation was made in the acetanilide monomer.[13]

In the low-frequency region of the REMPI spectrum up to 350 cm^{-1}, the peaks at 23.5, 49.6, 82.3, 129.5, and 177.1 cm^{-1}

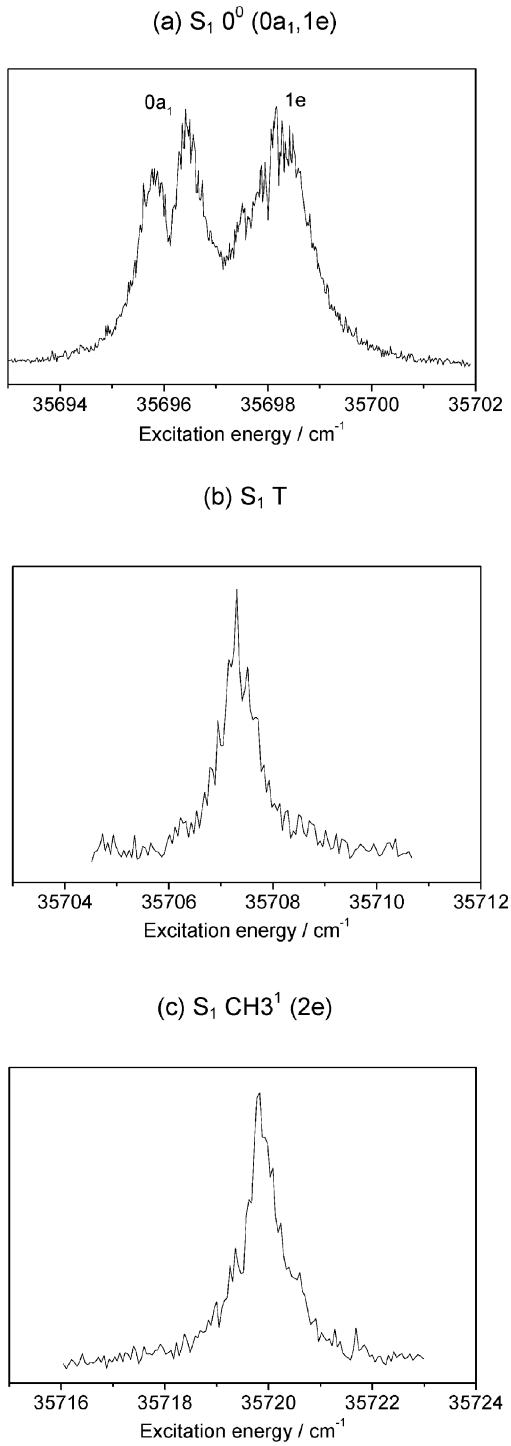

Figure 4. Comparison of band contours of (a) S_1 0^0, (b) S_1 T, and (c) S_1 $CH3^1$ (2e) bands.

above S_1 0^0 ($0a_1$) can be assigned to the methyl rotor excitations $CH3^1$ (2e), $CH3^2$ ($3a_1$), $CH3^2$ (4e), $CH3^3$ (5e), and $CH3^4$ ($6a_1$), respectively. The frequencies of those transitions are in excellent agreement to the simulated S_1 state rotor levels listed in Table 2 and show the anticipated rotational band contour; only the assignment of $CH3^4$ ($6a_1$) remains uncertain. The relatively low frequency of the S_1 state $CH3^1$ (2e) rotation in the complex is in agreement with the conclusion that the excited-state barrier height for internal rotation is very small, about 20 ± 5 cm^{-1}. Both a_1 rotor transitions, $CH3^2$ ($3a_1$) and $CH3^4$ ($6a_1$), show an additional feature immediately to their blue that cannot be assigned at present. In a manner similar to the acetanilide

TABLE 2: Experimentally Determined Methyl Rotor States of *trans*-Acetanilide·H_2O in the S_0, S_1, and D_0 States Compared to Simulated Eigenvalues[a]

assignment	experimental/cm^{-1}	simulated/cm^{-1}
S_0 state		B=5.2,V_3=50−60, V_6=0
$0a_1$	0	0
1e	2	2
S_1 state		B=5.2, V_3=20, V_6=0
$0a_1$	0	0
1e	5	4
2e	26	23
$3a_1$	50	49
4e	85	84
5e	132	131
$6a_1$	177	188
D_0 state		B=5.2, V_3=320, V_6=0
$0a_1$	0	0
1e	0	0
2e	103	108
$3a_1$	175	196
4e	208	204
5e	265	264

[a] All frequencies are given in cm^{-1} and relative to $CH3^0$ $0A_1$ of the corresponding state. B is the reduced internal rotor constant, and V_3 and V_6 are internal rotor barrier heights. See ref 13 for more details.

monomer, a progression of three, equally spaced (by ∼4 cm^{-1}) very weak vibrational features is built off the $CH3^3$ (5e) methyl rotation and has been assigned to the intermolecular out-of-plane bend, β'', which according to the ab initio calculations is the lowest frequency vibration, predicted at 14 cm^{-1}. The relatively small feature at 28.6 cm^{-1} above S_1 0^0 ($0a_1$) is analogously assigned to the combination band $CH3^1$ (2e) + β''. The lowest frequency feature in the REMPI spectrum at 11.1 cm^{-1} above the S_1 0^0 ($0a_1$) band is assigned to the side-chain torsion T, which was predicted to appear at 37 cm^{-1} by CASSCF calculations, for the following reasons: The forbidden (in C_s symmetry) torsion becomes allowed in the G_6 group due to coupling to the methyl group rotation, with the peak profile corresponding to an e ↔ e transition (Figure 4b). Furthermore, a feature was observed at a very similar frequency in the monomer spectrum (16 (S_0) and ∼14 cm^{-1}(S_1)). The low-frequency features now assigned to T, $CH3^1$ (2e) (Figure 4c) and $CH3^2$ ($3a_1$), were used as resonant intermediate levels for ZEKE spectra. The corresponding vibrations in the cationic spectrum show an enhancement in intensity which is in accord with a high $\Delta v = 0$ propensity. The remaining peaks can be assigned by comparison to the acetanilide monomer spectrum, which suggests that the peak of very weak intensity at 167 cm^{-1} is the in-plane side-chain bend, B′; this feature appears in the monomer REMPI spectrum at exactly the same frequency. No corresponding monomer peak was observed for the feature at 120 cm^{-1}, which was therefore assigned to the intermolecular stretch, σ. As expected from other hydrogen-bonded complexes, the stretch is of significant intensity. CASSCF/cc-pVDZ S_1 state calculations predict the σ and B′ vibrations to appear at 130 and 191 cm^{-1}, respectively. However, in the ab initio normal-mode analyses, both modes show a large degree of mixing. The lower frequency mode, labeled σ, corresponds to an out-of-phase, and the higher, labeled B′, corresponds to an in-phase movement of the water stretch displacement and side-chain bend. A similar coupling occurs for the out-of-plane bend, β'', and side-chain torsion T.

It should be noted that for both features, σ and B′, a_1 and e symmetry components appear with a $0a_1$−1e splitting of the S_1 bands of 2.1 cm^{-1} compared to a splitting of 2.3 cm^{-1} for the S_1 0^0 transition. This indicates that σ and B′ vibrational

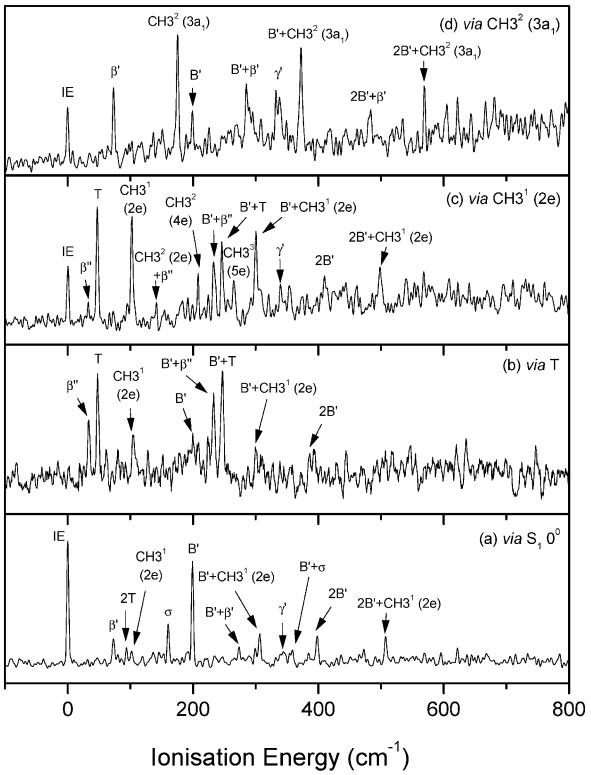

Figure 5. ZEKE spectra of *trans*-acetanilide·H_2O recorded via the (a) S_1 0^0, (b) side-chain torsion T, and methyl group internal rotations (c) $CH3^1$ (2e) and (d) $CH3^2$ ($3a_1$). All spectra are displayed relative to their respective ionization energy (IE) from either the S_0 0_0 ($0a_1$) or S_0 0_0 (1e) level. For exact ionization energy values see Table 3.

excitation slightly increases the S_1 state barrier height for methyl group rotation. A further noteworthy observation is that, whereas the $0a_1$ and 1e peak intensities of the S_1 0^0 band are very similar, for S_1 σ the intensity of both symmetry components is considerably different. Unfortunately, the resolution of the S_1 $\sigma \leftarrow S_0$ 0^0 band in spectrum Figure 2 is not good enough to unambiguously identify the symmetry of both components and determine the barrier height changes exactly. An assignment of 1e and $0a_1$ species in reversed order would be possible in principle, although it would imply an increase in S_1 state methyl rotor barrier height by ∼200 cm^{-1} under additional excitation of the intermolecular stretch, σ. Such an assignment is therefore considered less likely.

3.3. ZEKE Spectra of *trans*-Acetanilide·H_2O. The ZEKE spectra of the NH-bound water complex recorded via the (a) S_1 0^0, (b) side-chain torsion T, and methyl group internal rotations (c) $CH3^1$ (2e) and (d) $CH3^2$ ($3a_1$) are displayed in Figure 5, with peak positions listed in Table 3. The ionization energy was determined as 62 633 ± 5 cm^{-1} which corresponds to a red shift of 2904 ± 5 cm^{-1} with respect to the monomer ionization energy. The CASSCF calculations predict an ionization energy and red shift of 53 388 and 3482 cm^{-1} (62 040 and 3246 cm^{-1} including MP2 and ZPE corrections), respectively.

The methyl group internal rotations appear in the complex at very similar frequencies as in the monomer so that the barrier can be assumed to be of similar height in both species. The eigenvalues of methyl rotor levels in a V_3−V_6 potential were simulated to confirm the assignment in Table 3 and determine the barrier height accurately. The best agreement was achieved for a barrier height of 320 cm^{-1} for V_3; all values are summarized in Table 2. This barrier height of 320 cm^{-1} implies that the $CH3^0$ ($0a_1$) and $CH3^0$ (1e) levels of the D_0 state are

TABLE 3: Vibrational Frequencies in cm^{-1} Observed in the ZEKE Spectra of *trans*-Acetanilide·H_2O Recorded via the (a) S_1 0^0, (b) Side-Chain Torsion T, and Methyl Group Internal Rotations (c) $CH3^1$ (2e) and (d) $CH3^2$ ($3a_1$)[a]

relative position/cm^{-1}					
(a) via S_1 0^0	(b) via T	(c) via $CH3^1$ (2e)	(d) via $CH3^2$ ($3a_1$)	assignments	CASSCF
0 s		0 m	0 m	IE	
(62632.0 ± 5)		(62632.2 ± 5)	(62634.4 ± 5)		
	34 m	33 vw		β''	23
	48 s	47 s		T	59
73 w			73 m	β'	79
94 vvw				2T	
102 vvw	104 w	103 s		$CH3^1$ (2e)	119
		(141 vw)		$CH3^1$ (2e)+ β''/$CH3^1$ (2e)+T	
160 m				ó	165
			175 s	$CH3^2$ ($3a_1$)	
199 s	200 w		199 w	B′	207
	209 w	208 w		$CH3^2$ (4e)	
	233 s	233 w		B′ +β''	
	247 s	246 m		B′ +T	
		265 w		$CH3^3$ (5e)	
273 vw				B′ +β'	
			285 w		
306 w	299 w	300 s		B′ +$CH3^1$ (2e)	
344 vw		340 vw	338 w	γ'	331
359 vw				B′+ σ	
			372 s	$CH3^2$ ($3a_1$)+ σ	
398 w	392 w	410 vw		2B′	
			484 w	2B′ +β'	
507 w		498 w		2B′+$CH3^1$ (2e)	
			570 w	2B′+σ	
824 vw					
887 vw					
		991 w			
1086 vw					

[a] Frequencies are given relative to their respective ionization energy (IE) from either the S_0 0_0 ($0a_1$) or S_0 0_0 (1e) level. Intensities are denoted as vvw = very very weak, vw = very weak, w = weak, m = medium, s = strong. Assignments and CASSCF/cc-pVDZ harmonic frequencies of the D_0 state are also presented.

(nearly) degenerate, which allows us to determine the ground-state splitting from the difference in ionization energies of the ZEKE spectra selectively recorded via intermediate levels of A and E symmetry. Comparison of the ionization energies of the ZEKE spectra via S_1 $CH3^1$ (2e) and S_1 $CH3^2$ ($3a_1$) indicates a splitting of 2.2 cm^{-1} for the $CH3^0$ ($0a_1$) and $CH3^0$ (1e) levels in the neutral ground state, S_0. Although the splitting is within the absolute error given for the ionization energies, relative values are expected to be more precise allowing the splitting to be determined within ±2 cm^{-1}. The fact that the $0a_1$ and 1e symmetry species in the S_1 0^0 origin band occur in this order with a splitting of 2.3 cm^{-1} means that the barrier height in the S_1 state is lower than in the S_0 state, and the S_1 rotor levels $CH3°$ ($0a_1$) and $CH3^1$ (1e) are separated by 5.5 cm^{-1}. Barrier heights in the S_0 and S_1 states were obtained as 55 and 20 cm^{-1}, respectively, from simulations of methyl rotor states of features observed in the REMPI spectrum. For the monomer, barrier heights of 10−30 cm^{-1} in the ground-state S_0 and 50 cm^{-1} in the excited-state S_1 were determined.[13]

According to CASSCF/cc-pVDZ calculations, complexation with water leads to reorientation (rotation by 60°) of the methyl group in the minimum energy configuration of the S_0 and S_1 states which might result in a change in barrier heights compared to the acetanilide monomer. In the cation, the orientation of the methyl group (one hydrogen toward the amide O) is identical for the monomer and the complex; that is, in the complex, the methyl group rotates by 60° upon ionization. These orientations of the methyl group were determined by ab initio calculations, although Fujii et al.[18] have demonstrated, for example, for cresol and cresol·H_2O how one-dimensional rotor simulations of the intensity patterns in ZEKE spectra provide information on the relative alignment of the methyl group from wave function overlaps between different states (e.g., S_1 and D_0) as a function of the rotation angle. If the methyl conformation changes by 60° upon ionization from S_1, one would intuitively expect transitions between low energy A_1 and E levels to appear with weak intensity. Transitions from methyl rotor levels near or above the barrier height of the S_1 state potential should show increasing overlap of initial and final state wave functions and therefore gain intensity. The relatively intense ionization energy band in the ZEKE spectrum of acetanilide·H_2O recorded via the S_1 0^0 intermediate level is at odds with the computationally predicted change in methyl conformation; consequently, it has to be considered that the CASSCF/cc-pVDZ predictions are probably at fault.

The ZEKE spectrum recorded via the S_1 0^0 origin is shown in Figure 5a. The main features are the cation band origin, a band at 199 cm^{-1} ion internal energy, and its overtone at 398 cm^{-1}. Both bands are assigned to the side-chain bend B′ and B′2, which also showed a progression in the corresponding monomer spectrum at 181 and 364 cm^{-1}. The observed increase in frequency upon complexation was also predicted by the CASSCF calculations and is most likely the result of the bending motion of the side-chain being hindered by the water molecule. The corresponding bending mode was observed in formanilide·H_2O at 221 cm^{-1}. Although other hydrogen bonded complexes such as phenol·H_2O,[19] resorcinol·H_2O,[20] and methoxyphenol·H_2O[21] would imply an assignment of the progression to the intermolecular stretch, σ, due the shortening in hydrogen bond distance upon ionization, the absence of such a progression in formanilide·H_2O[5] suggests that molecules with more flexible side-chains, e.g., *N*-phenylamides, show different multidimensional Franck−Condon overlaps. Further ab initio investigations would allow Franck−Condon simulations[22,23] of the ZEKE

spectra to try and understand a relation between simultaneous geometry changes of the side chain and hydrogen bond and resulting intensity patterns. Alternatively, the feature at 199 cm^{-1} could be assigned to the $CH3^2$ ($3a_1$) methyl rotor excitation, which would bring it into closer agreement with the simulated eigenvalue but would lead to difficulties in the assignments of the progressional features. The intermolecular stretch, σ, is expected to appear at least as an intense fundamental and is therefore assigned to the peak at 160 cm^{-1} ion internal energy. The CASSCF calculations predict a harmonic frequency of 165 cm^{-1} for σ, but an additional confirmation is gained from the appearance of the formanilide·H_2O^5 stretch at 174 cm^{-1}. Smaller features observed in the ZEKE spectrum of acetanilide·H_2O recorded via S_1 0^0 can be attributed to the intermolecular in-plane bend, β', which was also observed in formanilide·H_2O, the second quantum of the torsion, T^2, and the methyl group rotation, $CH3^1$ (2e). All lower wavenumber modes appear again as combination bands with the side-chain bend B′.

The ZEKE spectrum recorded via the intermediate side-chain torsion, T, is displayed in Figure 5b. The ionization energy peak does not gain any intensity, possibly because of Franck−Condon factors. The lowest energy peak observed corresponds to the intermolecular out-of-plane bend, β''. The appearance of this mode with considerable intensity can be explained by coupling of the water out-of-plane movement to the side-chain torsion, which was also observed in the CASSCF normal-mode analysis. The β'' vibration describes a motion where the side-chain and H_2O move in opposite directions, and the T vibration corresponds to their movement in the same direction. In accord with an anticipated $\Delta v = 0$ propensity, T is one of the most prominent peaks in the spectrum, whereas a relatively small $CH3^1$ (2e) rotation feature is also observed. Combination bands between these vibrations and the side-chain in-plane bend, B′, are also present, all of which correspond to G_6 only symmetry-allowed e ↔ e transitions.

The ZEKE spectrum recorded via the $CH3^1$ (2e) (Figure 5c) intermediate level shows a D_0 band origin feature of medium intensity. Again, predominantly e ↔ e transitions are observed throughout the spectrum. The most prominent features are the side-chain torsion T and internal rotation $CH3^1$ (2e). These modes and the intermolecular out-of-plane bend, β'', are observed as combination bands with B′.

The final ZEKE spectrum recorded via the methyl internal rotation $CH3^2$ ($3a_1$) (Figure 5d) displays, as expected, a slightly different pattern of vibrational features. Exclusively a_1 symmetry modes are present. The in-plane intermolecular bend, β', gains considerably intensity compared to the ZEKE spectrum recorded via S_1 0^0, but the most prominent peak is the $CH3^2$ ($3a_1$) methyl group rotation at 175 cm^{-1}. Combination bands between the above vibrations and B′ are also observed.

4. Conclusions

The hydrogen-bonded water complex of acetanilide has been investigated, and the results have been compared to both the acetanilide monomer and the formanilide·H_2O complex. The water was found to be attached to the amide N−H in common with the most stable water complex of formanilide; a CO-bound complex could not be identified. Excitation energies, ionization energies and their red shifts were determined to be 35 697 ± 2, 62 633 ± 5, 207 ± 2, and 2904 ± 5 cm^{-1}, respectively. This is slightly lower than the corresponding values of formanilide·H_2O, and it can therefore be concluded that the amide hydrogen in acetanilide gains relatively less acidity upon both electronic excitation and ionization. The intermolecular stretch was observed at a lower frequency than in formanilide·H_2O indicating a weaker hydrogen bond. In the REMPI spectrum of acetanilide·H_2O, no intermolecular in-plane bend, β', was observed, but the corresponding mode in the ZEKE spectrum appeared at a higher frequency than in formanilide·H_2O. This can be explained by steric hindrance of the methyl group neighboring the hydrogen bond site. Acetanilie·H_2O spectra also display prominent methyl rotor excitations. Barrier heights and eigenvalues were determined for the S_0, S_1, and D_0 states by simulations; compared to the monomer, the barrier height of the acetanilide·H_2O complex increased from 20 to 55 cm^{-1} in the S_0 state, decreased in the S_1 state from 52 to 20 cm^{-1}, and remained similar (320 cm^{-1}) in the D_0 state. All these results are in marked contrast to the van der Waals bound complex acetanalide·Ar.[24]

Acknowledgment. We thank the Engineering and Physical Sciences Research Council (EPSRC, Grant GR/M4845/) for financial support. The authors thank Xin Tong for his help with the experiment. We are most grateful to Masaaki Fujii (Okazaki) for providing us with his internal rotor fitting program. S.U. acknowledges support from the Fonds des Verbandes der Chemischen Industrie followed by a DAAD Doktorandenstipendium im Rahmen des gemeinsamen Hochschulsonderprogramms III von Bund und Ländern.

Supporting Information Available: Full geometries (Table A), excitation and ionization energies (Table B), CASSCF harmonic vibrational frequencies up to 1000 cm^{-1} (Table C), and Mulliken, ESP, and NPA charges calculated at the CASSCF/cc-pVDZ level of theory (Table D). This material is available free of charge via the Internet at http://pubs.acs.org.

References and Notes

(1) Manea, V. P.; Wilson, K. J.; Cable, J. R. *J. Am. Chem. Soc*. **1997**, *119*, 2033.

(2) Ullrich, S.; Tarczay, G.; Tong, X.; Dessent, C. E. H.; Müller-Dethlefs, K. *Angew. Chem. Int. Ed., Commun.* **2002**, *41*, 166.

(3) Ullrich, S.; Tarczay, G.; Tong, X.; Dessent, C. E. H.; Müller-Dethlefs, K. *Phys. Chem. Chem. Phys.* **2001**, *3*, 5450.

(4) Mons, M.; Dimicoli, I.; Tardivel, B.; Piuzzi, F.; Robertson, E. G.; Simons, J. P. *J. Phys. Chem. A* **2001**, *105*, 969.

(5) Robertson, E.; Simons, J. P. *Phys. Chem. Chem. Phys.* **2001**, *3*, 1.

(6) Fedorov, A. V.; Cable, J. R. *J. Phys. Chem. A* **2000**, *104*, 4943.

(7) Dickinson, J. A.; Hockrodge, M. R.; Robertson, E. G.; Simons, J. P. *J. Phys. Chem. A* **1999**, *103*, 6938.

(8) Ullrich, S.; Tarczay, G.; Tong, X.; Ford, M. S.; Dessent, C. E. H.; Müller-Dethlefs, K. *Chem. Phys. Lett.* **2002**, *351*, 121.

(9) The program used for the simulation of the methyl rotor eigenvalues was written by Dr. Ken Takazawa based on the paper of Lewis, J. P.; Laane, J.; *J. Mol. Struct*. **1972**, *12*, 427. Prof. M. Fujii's (Institute for Molecular Sciences, Okazaki) assistance is greatly acknowledged.

(10) Haines, S. R.; Geppert, W. D.; Chapman, D. M.; Watkins, M.; Dessent, C. E. H.; Cockett; M. C. R.; Müller-Dethlefs, K. *J. Chem. Phys.* **1998**, *109*, 9249.

(11) Dessent, C. E. H.; Müller-Dethlefs, K. *Chem. Rev.* **2000**, *100*, 3999.

(12) Frisch, M. J.; Trucks, G. W.; Schlegel, H. B.; Scuseria, G. E.; Robb, M. A.; Cheeseman, J. R.; Zakrzewski, V. G.; Montgomery, J. A., Jr.; Stratmann, R. E.; Burant, J. C.; Dapprich, S.; Millam, J. M.; Daniels, A. D.; Kudin, K. N.; Strain, M. C.; Farkas, O.; Tomasi, J.; Barone, V.; Cossi, M.; Cammi, R.; Mennucci, B.; Pomelli, C.; Adamo, C.; Clifford, S.; Ochterski, J.; Petersson, G. A.; Ayala, P. Y.; Cui, Q.; Morokuma, K.; Malick, D. K.; Rabuck, A. D.; Raghavachari, K.; Foresman, J. B.; Cioslowski, J.; Ortiz, J. V.; Stefanov, B. B.; Liu, G.; Liashenko, A.; Piskorz, P.; Komaromi, I.; Gomperts, R.; Martin, R. L.; Fox, D. J.; Keith, T.; Al-Laham, M. A.; Peng, C. Y.; Nanayakkara, A.; Gonzalez, C.; Challacombe, M.; Gill, P. M. W.; Johnson, B. G.; Chen, W.; Wong, M. W.; Andres, J. L.; Head-Gordon, M.; Replogle, E. S.; Pople, J. A. *Gaussian 98*, revision A.7; Gaussian, Inc.: Pittsburgh, PA, 1998.

(13) Ullrich, S.; Müller-Dethlefs, K. *J. Phys. Chem. A* **2002**, *106*, 9181.

(14) Ullrich, S.; Müller-Dethlefs, K.; Knowles, P. J. *Phys. Chem. Chem. Phys*. To be submitted.

(15) Samdal, S. *J. Mol. Struct.* **1998**, *440*, 165.

(16) Wilson, E. B. *Phys. Rev.* **1934**, *45*, 706.
(17) Roth, W.; Imhof, P.; Gerhards, M.; Schumm, S.; Kleinermanns, K. *Chem. Phys.* **2000**, *252*, 247.
(18) Suzuki, K.; Ishiuchi, S.-I.; Fujii, M. *Faraday Discuss*. **2000**, *115*, 229.
(19) Dopfer, O.; Reiser, G.; Müller-Dethlefs, K.; Schlag, E. W.; Colson, S. D. *J. Chem. Phys.* **1994**, *101*, 974.
(20) Geppert, W. D.; Dessent, C. E. H.; Ullrich, S.; Müller-Dethlefs, K. *J. Phys. Chem. A* **1999**, *103*, 7186.
(21) Geppert, W. D.; Ullrich, S.; Dessent, C. E. H.; Müller-Dethlefs, K. *J. Phys. Chem. A* **2000**, *104*, 11864.
(22) Schumm, S.; Gerhards, M.; Kleinermanns, K. *J. Phys. Chem. A* **2000**, *104*, 10648.
(23) Negri, F.; Zgierski, M. Z. *J. Chem. Phys.* **1997**, *107*, 4827.
(24) Tong, X.; Ullrich, S.; Dessent, C. E. H. Dessent; Müller-Dethlefs, K. *Phys. Chem. Chem. Phys.* **2002**, *4*.